Development of All Dry Nanoimprint Lift-Off Process for Growth of Nanowires

Yasna Aberi

Thesis for the Degree of Master of Science in Physics

2013

Supervisor: Ivan Maximov
Division of Solid State Physics
Department of Physics
Lund University
Lund, Sweden

Acknowledgments

First of all, I would like to thank my supervisor Ivan Maximov for his invaluable suggestions and discussions and also for his kindness and support during this project. I am very grateful to Mariusz Graczyk for his great ideas and discussions. Thanks also for his teaching and kindly help during the lab work. I learnt a lot from him.

I would like to thank the people from Obducat AB specially Babak Heidari for their help and advice. I am thankful to Andres Kvennefors, George Rydnemalm and Håkan Lapovski for their kind help at Lund Nano Lab. I thank Alexander Berg and Jesper Wallentin for growing the nanowires used in this project.

I sincerely thank my aunt Shaida and my uncle Mansor for their kindness and their purely support during my study in Sweden.
My parents, who supported me with kindness and love. I can always count on you whatever happens, thank you so much.

Contents

Popular Science iii

Abstract v

Abbreviations and Acronyms vii

1 Introduction 1

2 Nanofabrication 3

2.1 Nanofabrication by Lithography …………………………….. 4
2.1.1 Optical Lithography …………………………………… 4
2.1.1.1 Extreme Ultraviolet Lithography …………… 5
2.1.2 Electron Beam Lithography …………………………… 6
2.1.3 Nanoimprint Lithography ……………………….......... 8
2.1.3.1 Thermal Nanoimprint Lithography…………… 8
2.1.3.2 UV Nanoimprint Lithography ………………. 9
2.1.3.3 IPS-STU Nanoimprint Lithography ………… 10
2.1.3.4 Mold Fabrication ……………………………. 10
2.1.3.5 NIL Resist …………………………………… 12
2.2 Nanofabrication By Etching ………………………………… 13
2.2.1 wet etching ……………………………………………… 13
2.2.2 Dry Etching ……………………………………………… 14
2.2.2.1 Reactive Ion Etching ………………………… 14
2.3 Nanowire Growth …………………………………………… 16
2.3.1 InP Nanowires ……………………………………….. 17
2.3.2 Gold Seeded Nanowire Growth ……………………… 17
2.3.3 Metal-Organic vapor Phase Epitaxy ………………… 17

3 Experimental 19

3.1 IPS-STU NIL Lift-Off Process ……………………………… 21
3.1.1 Combination of Double Layers Resist ………………... 21
3.1.2 IPS-STU Nanoimprint Process ………………………. 22
3.1.3 RIE-O_2 plasma ……………………………………….. 23
3.1.4 Metallization and Lift-Off ………………………........ 25
3.2 Nanowire Growth …………………………………………… 27
3.3 Characterization Method ……………………………………. 29
3.3.1 Scanning Electron Microscopy ……………….............. 29
3.3.2 Ellipsometry …………………………………………... 30

4 Results and Discussion **31**
4.1 Investigation of Etch Rate ………………………………. 31
4.2 Dry Etching Process Results of NIL Samples ………….. 32
4.3 Lift-Off Process Results ………………………………... 34
4.4 Nanowire Growth Results ………………………………. 36

5 Conclusions and Outlook **41**

Appendix I **43**

Bibliography **45**

Popular Science

There are two methods for fabrication of nanostructures: bottom-up and top-down. In this work IPS-STU nanoimprint process that is a top-down approach is applied to pattern the substrate. A dry etching process is developed to realize a desired undercut in the resist for the lift-off. Gold particles are produced on the surface, which could be used to grow InP nanowires (NWs) using epitaxial techniques.

Nanoimprint lithography (NIL) is one of the lithographic methods. In this process the features of a Ni stamp as a master stamp are transferred into the underlying substrate mechanically. This technique leads to high throughput and high resolution.

There are two approaches to make a desired undercut in the resist. One approach is a wet etching process, which uses O_2 plasma and MF319 solvent as etching developer to create undercut in the resist. Wet etching process does not affect the size of holes. However adhesion and difficulties to control the process manually are the main disadvantages. Another approach employs the dry etching process. This process uses O_2 plasma to make undercut in the resist, although having the disadvantage of affecting the size of holes.

By performing epitaxial methods such as Metal-Organic Vapor Phase Epitaxy that is a bottom-up approach, NWs are grown. NWs are 1D structures with a diameter of few nanometers and a length of several micrometers. Due to their optical and electrical properties they are used in devices such as light-emitting diodes and transistors.

The results indicated that by optimizing RIE-O_2 plasma parameters the desired undercuts in the bottom layer resist are realized. The controlled diameter of gold particles could be obtained and also, dry etching works well to grow InP NWs from gold particles shown in Fig. 1.

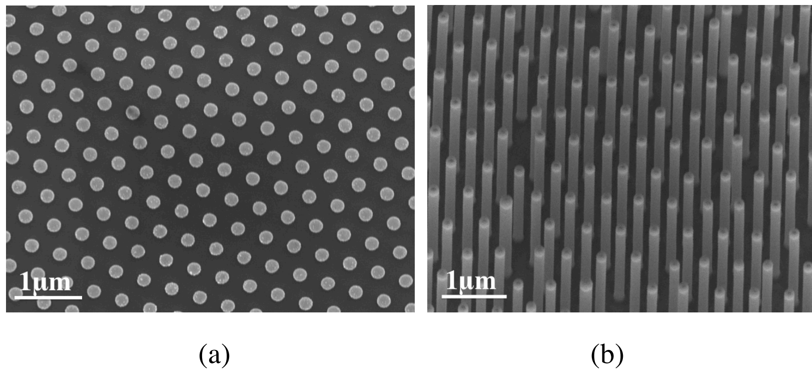

Figure 1: (a) Gold particles produced on the surface directly after lift-off, (b) Grown of InP NWs by using a dry etching process.

Abstract

In this project, nanoimprint lithography has been applied to define gold particles on the surface of an InP wafer. For achieving this aim, a dry etching process has been developed to create resist undercut for the lift-off. In order to prepare the required undercuts, RIE parameters were optimized and desired undercuts were made at etch times of 80 s to 120 s. Also, to obtain anisotropy and high etch selectivity, etch rate test of a best combination of polymer layer materials was investigated. Lift-off was realized and gold particles were deposited on predefined position on imprinted surface.

Gold-seeded InP nanowires have been grown using metal-organic vapour phase epitaxy. Characterization by scanning electron microscope after growth demonstrated the high tendency of gold particles to move during epitaxial growth. Gold particles were merged together on the surface due to the presences of InP oxide induced by O_2 plasma used in dry etching. Wet chemical treatment by using diluted HF and HCl solutions was applied to remove the InP oxide on the surface. The influence of wet chemical treatment to reduce the merging of gold particles and to improve the growth of nanowires was investigated. It was indicated that nanowires grew much better on the surface treated by a diluted HF solution. On the HF treated surface the smallest number of gold particles merged together resulting in nearly uniform InP nanowires grown on controlled position. The distribution of grown nanowires as diameter versus amount was plotted as a histogram and the behavior of nanowires grown was studied.

Abbreviations and Acronyms

AFM	Atomic force microscope
CBE	Chemical beam epitaxy
CD	Critical dimension
EUVL	Extreme ultra violet lithography
EBL	Electron beam lithography
FIB	Focused ion beam
IC	Integrated circuit
IPS	Intermediate polymer stamp
IPA	Isopropanol
MOVPE	Metal- organic vapor phase epitaxy
MBE	Molecular beam epitaxy
NIL	Nanoimprint lithography
NW	Nanowire
PMMA	Polymethymetacrylate
RIE	Reactive ion etching
RF	Radio frequency
SCCM	Standard cubic centimeters per minute
STU	Simultaneous thermal ultra violet
SAM	Self assembled monolayer
STI	Shallow trench isolation
SEM	Scanning electron microscope
T_g	Glass transition temperature
TU_2	Imprint resist
UV	Ultra violet
UVL	Ultra violet lithography
ZEP	Organic resist

CHAPTER 1
Introduction

Nanotechnology has become a promising technology during the last few years. Nanotechnology as a multidisciplinary field has a lot of potential applications for physics, chemistry, biology, medical and electronic purposes [1]. Different aspects of nanotechnology and nanoscience including nanoelectronics, nanobiology and nanophotonics have become one of the main areas of academic and industrial research. Making and controlling the structures at 1-100 nm dimensions is the main outcome of nanotechnology and nanoscience.

There is an increasing demand for scaling down in many fields of technology. Manufacturing of smaller transistors and higher density integrated circuits (ICs) in semiconductor industry [2] has become a main motivation of miniaturization.

There are two approaches for fabrication of such structures in dimension of nanoscale: bottom-up and top-down. In bottom-up method atoms or molecules are assembled to the structures. In top-down approach a lithography method is used to transfer patterns into the substrate. UV lithography, electron beam lithography (EBL) and ion beam lithography are the most common lithography techniques that fulfill the requirements of resolution and throughput. Nanoimprint lithography (NIL) is another lithography method that has been developed in the last few years due to its simplicity, high throughput, low cost, high resolution and potential new applications [3].

One of the processes in nanofabrication of devices is etching. Etching processes remove mask material selectivity from the substrate. There are two approaches to etching: wet chemical etching and dry etching. Due to some disadvantages of wet chemical etching process such as poor stability and reproducibility and the risk of handling chemicals manually [4] a dry etching process has been developed. In dry etching process O_2 plasma is used to create surface reaction chemically and physically.

This thesis deals with the development of all dry nanoimprint lift-off process in order to create a desired undercut in the resist for the lift-off. Dry etching process is developed to produce gold particles on the surface and then growth of nanowires (NWs). This thesis includes following parts: Chapter 2 gives an overview of nanofabrication. The experimental processing and fabrication methods are described in chapter 3. The results are discussed in chapter 4. Finally Chapter 5 concludes this work and gives an outlook of this study.

CHAPTER 2
Nanofabrication

Shrinking of feature sizes in semiconductor industry particularly in manufacturing of ICs has become a driving force to fabrication of transistors and other IC components with nano dimensions [1].

Nanofabrication is the design and manufacturing of structures at 1-100 nm sizes, which is emerged from microfabrication at this dimensional scale.

According to Moore's law the density of transistors on a chip in every 18 months can be doubled. However, nowadays the miniaturizing of the IC structure has led the minimum feature size of an IC of 22 nm. In comparison with a few years ago, where the minimum feature size of an IC was 250 nm [1]. This efficiency to reduce the feature size of ICs was possible due to advances in lithographic technology.

2.1 Nanofabrication by Lithography

Lithography is one of the key technology for the semiconductor industry. As mentioned before, by using lithography and etching techniques, the pattern is transferred into the substrate. Lithographic techniques result in cost reduction in IC production [5]. There are a number of requirements for lithography including resolution, critical dimension (CD) control and throughput. In this section the current lithography methods are discussed.

2.1.1 Optical Lithography

The main lithography method to achieve ever- smaller structures with high production volume and costs as low as possible is optical lithography [6]. In optical lithography the features are transferred to photoresist layer by using ultraviolet light. Printing is referred as a process that projects the image of the features onto the substrate using a light source and photomask [7].

Two types of printing are shadow printing and projection printing as shown in Fig. 2.1. Shadow printing consists of contact printing and proximity printing. Contact printing is the direct contact between photomask and resist coated substrate by exposing resist. The resolution achieved by this process is less than 1 μm. However, the direct contact reduces the uniformity of achieved resolution across the substrate. Also, contact printing leaves defects in the masks and the substrates [8]. Proximity printing is known as close proximity between the mask and the substrate. The mask used in this technique has a longer lifetime compared to that used in contact printing. In projection printing there is a gap between the mask and the substrate.

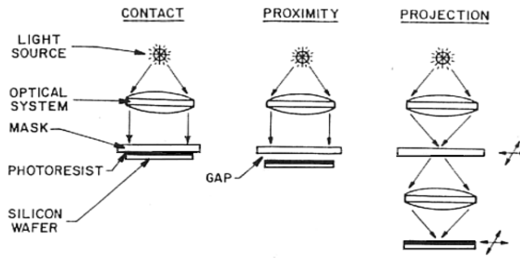

Figure 2.1: Schematic images of UV lithography [32].

2.1.1.1 Extreme Ultraviolet Lithography

To reach 32 nm line widths in IC fabrication, extreme ultraviolet lithography (EUV) is used [6]. The wavelength of the extreme ultraviolet light used in this technique is 10-14 nm. This wavelength allows high resolution. An EUV system uses multilayer mirrors as reflective element. EUV is generated by using a plasma or a synchrotron source. The exposure system is based on an image reduction so that the mask, illuminated by the source, is projected onto the substrate and the size of the patterns is reduced accordingly. High throughput is an advantage of the EUV lithography. A schematic diagram of the EUV system illustrated in Fig. 2.2.

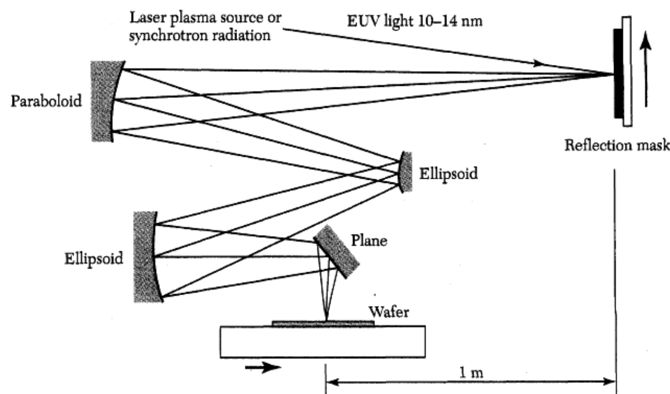

Figure 2.2: Schematic diagram of EUV setup [8].

2.1.2 Electron Beam Lithography

Electron beam lithography (EBL) is one of the widely used lithography techniques in nano-research, which benefits from a highly focused electron beam for creating nano-scale features.

Contrary to the conventional UV lithography where the resolution is limited by the wavelength of light and its diffraction, the very small spot size of an e-beam leads to an excellent resolution (less than 10 nm) [9]. Many applications such as electrical connection of individual molecules or single electron devices [10] need to be produced in sub -10 nm structures. However, EBL has not yet taken the place of the optical lithography due to very low throughput, which makes it an inefficient method for mass fabrication.

There are some advantages of EBL such as high resolution compared to the optical lithography. Due to the fact that the patterns are written directly onto the resist, there is no need to use a mask. Moreover, a variety of resists including organic (e.g. PMMA and ZEP) and inorganic (e.g. HSQ) resists [11] can be used in EBL.

There are however disadvantages for EBL technique. In this technique the resolution is limited by the generation of backscattered electrons and the proximity effect. The proximity effect results in the overexposure of the small features located near each other or in close proximity of a large feature. It leads to loss of contrast for those features. Other disadvantages are the complexity and high cost of the EBL system.

A schematic of the EBL illustrated in Fig. 2.3. The EBL system includes an electron source, an e-beam column on SEM and a stage located in a vacuum chamber.

Loading and unloading the sample, the exposure setting, beam deflection and alignment and the vacuum conditions are all controlled by the computer. The pattern is also written in computer software.

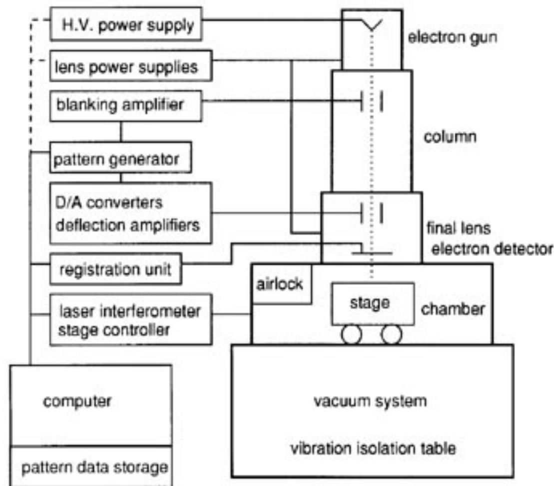

Figure 2.3: A schematic diagram of EBL setup [12].

The basic principle of EBL is similar to that of the optical lithography. The sample is coated with an e-beam sensitive resist layer (positive or negative). Upon exposing the regions of the resist defined by the pattern, chain scission of the positive resist or cross-linking of the negative resist in those regions happens. Thus, the pattern is transferred to the resist and then to the substrate by subsequent etching. The e-beam patterns the resist either by raster or by vector scanning. In the former mode, the beam scans entire area of the writing field and generates the pattern by blanking the beam on/off whereas in vector scan or projection mode after exposing a feature, the beam jumps to another one.

An efficient EBL system must fulfill several criteria [11]. First, the spot size of the e-beam needs to be a few nm. Next, high throughput and low cost are desirable factors. Finally, it should be capable of writing large areas in a reasonable amount of time.

2.1.3 Nanoimprint Lithography

Nanoimprint lithography (NIL) is a nonconventional patterning process. In this technique a mold with patterned structures is pressed mechanically into a resist layer material. The mold nanoscale pattern is transferred into the material by replication. Nanoimprint lithography was proposed by Stephen Chou et al. [13] in 1996, to overcome the problems encountered by the diffraction or scattering of beam in the optical lithography technique. Nowadays, fabrication of sub-50 nm structures can be achieved by performing Nanoimprint lithography [14]. High resolution, high throughput, low cost and high fidelity in transferring nanoscale structures make NIL a potential candidate for a number of application such as photoelectric devices, microfluidic channels optical components, biosensors and nanowires [1,13,14,15]. The principle of NIL can be explained into three steps, (1) mold fabrication, (2) imprint process, (3) etching.

The following describes the main NIL techniques and the elements required for NIL such as mold fabrication and resist material.

2.1.3.1 Thermal Nanoimprint Lithography

In hot embossing or thermal nanoimprint lithography technique, the polymer resist is heated above its glass transition temperature (T_g). Then the mold, is pressed into the thermoplastic resist by applying high pressure. The mold is made of hard material with high resistance against pressure and temperature. Before removing the mold the temperature is decreased below,

T_g and the substrate must be cooled down. The mold is then released to transfer the pattern into the resist. The remaining residual layer will be removed by O_2 plasma ashing. Fig. 2.4 illustrates a schematic of the basic steps of thermal nanoimprint lithography.

2.1.3.2 UV Nanoimprint Lithography

The UV-Nanoimprint lithography is performed at low imprint pressure and room temperature by using UV light and a transparent mold. The mold is pressed into the UV curable resist. The UV curable resists have a number of properties such as low viscosity to fill quickly in the stamp cavity, fast UV curing and high dry etching selectivity [1]. After separating the mold, the remaining residual resist in the compressed area is removed via an etching process. Basic steps of UV-NIL are schematically illustrated in Fig. 2.4. High resolution, high speed patterning [8] and less time consuming in comparison to the thermal NIL are the advantages of the UV NIL technique.

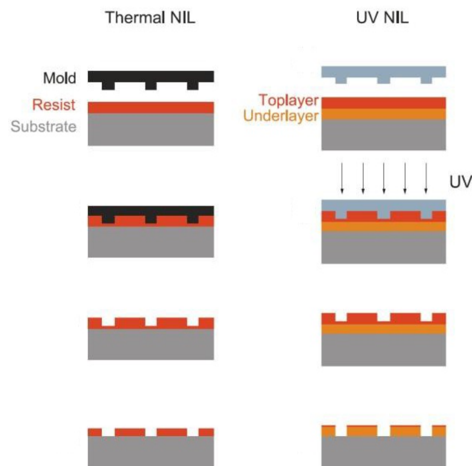

Figure 2.4: Schematic illustaration of thermal and UV nanoimprint lithography [15].

2.1.3.3 IPS-STU Nanoimprint Lithography

In the IPS-STU process an intermediate polymer stamp (IPS) is combined with simoltenous thermal and UV NIL (STU). This process is performed by two steps. First the features of a master stamp are replicated into a plastic polymer stamp called IPS. In the second step the current IPS is placed on a spin coated substrate with UV curable thermoplastic resists by applying simultaneous thermal and UV NIL at constant temprerature and pressure. After separation the pattern is transferred into the underlying substrate.

IPS enables contamination control and increases the master stamp life time hence, no direct contact between the master stamp and the substrate [8]. This method covers the problems related to different thermal expansion in stamp and substrate materials.

2.1.3.4 Mold Fabrication

Mold fabrication and its treatment are the requisites for the nanoimprint lithography. A high resolution mold results in a high resolution NIL; therefore the mold has the important role to replicate nanoscale features in the resist material. Solid materials with high strength and stability [2] can be used as NIL mold. Material properties such as hardness, compatibility and thermal expansion coefficient must be considered for selection mold material. For NIL processes where temperature is more than 100°C, the thermal expansion coefficient plays an important role. A thermal mismatch between the mold and the substrate can result in pattern distortions. Si, SiO_2, Ni, SiC, Si_3N_4, metals and diamond can be selected as mold for nanoimprint lithography [1, 2, 13]. An excellent mold is made of nickel because the Ni stamps are easy to replicate compared to those made of silicon.

Fabrication of a mold is started by spin coating the mold substrate with a resist, followed by lithography to create the mold feature. Fig. 2.5 illustrates the processing steps of mold fabrication. There are lithography methods such as UV lithography, EBL, AFM and FIB [8] to define the mold pattern; UV lithography for large structures and EBL for small structures are most common. After formation of the nanostructures on the resist material by exposure and transferring onto the mold substrate, a layer of metal is deposited on patterned resist, lift off process is performed to define the metal pattern and a patterned mask layer remains on the substrate. Then an anisotropic RIE process is carried out to etch the unwanted area [2]. By using EBL and lift off process a mold with 10 nm diameter arrays can be fabricated as shown in Fig. 2.6.

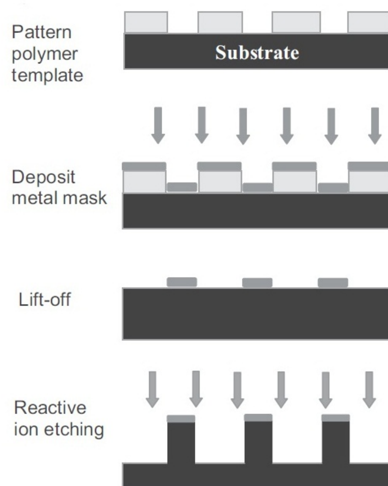

Figure 2.5: Schematic of mold fabrication process [2].

There is a strong adhesion between the mold and the surface of the resist. This adhesion results in defects and decreases the mold lifetime. To avoid this problem anti sticking treatment is required.

Anti-adhesive layers with low surface energy can be applied to coat the mold. A self–assembled monolayer (SAM) of 1H, 1H, 2H, 2H-perfluorodecyltrichlorosilane formed by liquid phase or vapor phase reaction can be deposited on the mold surface to reduce its surface energy.

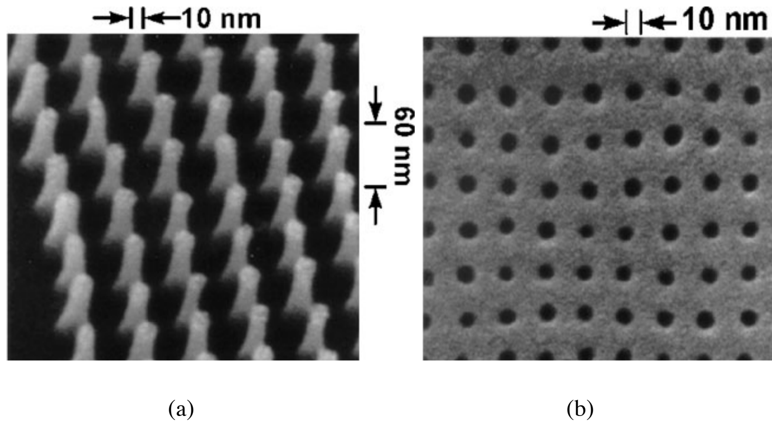

(a) (b)

Figure 2.6: (a) SEM image of a made mold with a 10 nm diameter array. (b) SEM image of hole arrays in PMMA by using such a mold [2].

2.1.3.5 NIL Resist

The resolution capability of the stamp can be realized with the nanoimprinting resists [1]. There are a number of properties for the resist material such as low imprinting temperature, low viscosity, low shrinkage and high resistance to etching [1, 2, 13]. However, a number of parameters such as the heating temperature, the applied pressure, the thickness of imprinting layers and the feature size of the stamp must be considered during the nanoimprint process.

Thermoplastic resists such as polymethylmethacrylate (PMMA), which is the commonly used EBL resist are excellent for NIL. They have good mechanical integrity and the possibility of low pressure imprinting. UV curable resists are liquid precursors cured by UV light that can be used in NIL as well since they satisfy the NIL resist requirements mentioned above.

2.2 Nanofabrication by Etching Technique

Etching in micro and nano fabrication is used to remove the substrate material through the mask. All the etching processes have two important etching characteristics: the isotropy/anisotropy of etching and the etch selectivity. Transferring the mask patterns into the substrate is the purpose of the etching [1]. The etching process of removing the substrate material with the same etching rate in all directions is called isotropic etching creating an undercut in the mask. Etching is termed anisotropic if the etching rate is different in the horizontal direction as compared to the vertical direction. Fig. 2.7 illustrates the difference between the isotropic and anisotropic etching. Another parameter that characterizes the etching techniques is etch selectivity referring to the etching rate ratio between substrate and the mask or the underlying layer.

In this section two types of etching techniques are described: the wet etching and the dry etching.

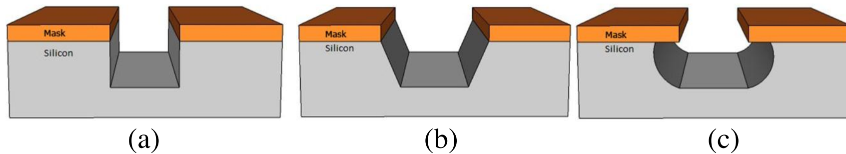

Figure 2.7: (a) Vertical wall, completely anisotropic etching, (b) Sloped wall, partially anisotropic etching, (c) Isotropic etching [17].

2.2.1 Wet Etching

Wet chemical etching is a process that uses liquid chemicals to selectivity remove parts of the substrate. Wet etching is typically isotropic. However, for a crystalline material that depends on crystalline orientation anisotropic wet etching is used [1]. This process results in the pattern etched larger than the mask pattern and for this reason, wet chemical etching is not

capable of high-resolution pattern transfer [1]. However, this etching process has a number of advantages such as a high etching rate compared to the dry etching process and a good selectivity for most material.

2.2.2 Dry Etching

To overcome the problems associated with wet etching and keep the fidelity to the mask, dry etching is employed. The capabilities of dry etching was first used by Irving [18, 19]. Dry etching is generally an anisotropic process. Dry etching uses the plasma under high energy ion bombardment to remove the substrate material. The process can be physical, chemical or a combination of physical and chemical etching including plasma etching, reactive ion etching (RIE), sputter etching, magnetically enhanced RIE [20]. In this work the focus is on RIE.

2.2.2.1 Reactive Ion Etching

To achieve critical dimensions down to or below 100 nm RIE is performed. RIE is the most widely used plasma etching process and is a chemical /physical approach developed by Hosokawa *et al.* in 1974 [21]. A number of applications exist such as the contact etching to form the gate stack etching and forming a shallow trench isolation (STI) [4] using RIE technology.

Directional high energy reactive species generated in the plasma react chemically with the surface simultaneous with physical effects created by ion sputtering. The shape of the etching profile as well as the degree of anisotropy are determined by the flux of these highly energetic ions [22]. The etching mechanism is illustrated in Fig. 2.8. Typical RIE gases are halogen containing gasses such as fluorine, chlorine and bromine [1] to

generate a plasma under the vacuum condition by an electromagnetic field. However, the requirements of a specific application play an important role for selecting a special gas.

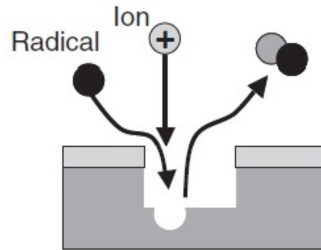

Figure 2.8: Schematic of RIE mechanism [4].

A typical RIE tool consists of a vacuum chamber. The vacuum chamber consists of two parallel plate electrodes driven by a radio frequency (RF) power as illustrated in Fig. 2.9. A negative DC bias is formed on the powered electrode (cathode) and the anode is grounded. The substrate placed on the cathode is bombarded with energetic positive ions. During the RIE the substrate surface is to be exposed to the high energy ion bombardment; one reason is the large negative potentials generated on the cathode [22]. Another reason is the low operating pressure of 10^{-3}-10^{-1} Torr in the RIE.

The RIE factors such as the RF power, the gas flow rate and the chamber pressure can be controlled and adjusted experimentally. By matching these parameters with quality markers such as anisotropy, selectivity and a desired result of etch rate, the RIE process can be controlled [1].

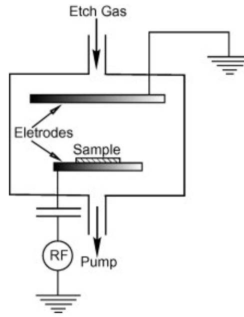

Figure 2.9: Schematic diagram of the RIE system [23].

2.3 Nanowire Growth

The early research on semiconductor nanowires (NWs) was started in 1990s [24]. The nanowires are aimed to be used for applications such as photonic, sensing and optoelectronics. NWs are 1D structures having diameters of few nanometers and lengths of several micrometers. NWs are fabricated using the bottom-up fabrication technique.

The electrical and optical capabilities of NWs and their property of high surface to volume has increased the attention in the growth of nanowires. The possibility of combinations of lattice mismatched materials is a big advantage of nanowires. Nowadays there are a number of nanowire-based devices, such as light-emitting diodes, transistors and solar cells [25, 26]. One of the most common techniques for growing semiconductor NWs is the particle- assisted growth.

InP nanowires used for this work are grown using gold particles in a MOVPE chamber.

2.3.1 InP Nanowires

Photovoltaic devices such as solar cells have recently become a focus of interest as they improve light trapping [27]. Nanowire based solar cells have a high efficiency of light absorption. InP NWs can be used to fabricate solar cells due to a direct band gap of 1.34 eV, which allows the absorption of light of solar spectrum wavelength [27]. It has been demonstrated that the efficiency the InP nanowire based-solar cells is as high as 13.8% while covering about 12% of the surface of a device [27].

2.3.2 Gold Seeded Nanowire Growth

Gold is the most common particle material used in the particle assisted nanowire growth. Gold has useful properties that match with a broad range of materials for nanowire growth and growth conditions [26], which make gold a proper candidate for a seed particle in the growth. Gold particles are defined by a lithography technique and deposited on a substrate surface. The preferred substrate surface orientation is often (111) B, however, other surface orientations can be used. After depositing the seed particles, the substrate is transferred to the MOVPE chamber.

2.3.3 Metal-Organic Vapor Phase Epitaxy

Metal-Organic Vapor Phase Epitaxy (MOVPE) is the widely used epitaxial technique for the growth of NWs. One advantage of MOVPE is its high throughput compared to other two epitaxial techniques; Molecular Beam Epitaxy (MBE) and Chemical Beam Epitaxy (CBE). The growth depends on parameters such as the chamber pressure, the molar fraction of the precursors, the substrate temperature and the gas flow [26].

The main components of the MOVPE system are the reactor, the heater and the plumbing system consisted of the valve system and the flow and pressure control. The substrate is placed on a susceptor inside the reactor chamber. The susceptor is heated using radio frequency coils or infrared lamps. At the certain temperature the precursors are mixed and the growth is performed.

CHAPTER 3
Experimental

The current intermediate polymer stamp-simultaneous thermal and UV imprint (IPS-STU) process is based on the use of a double layer resist system to create a negative slope in the resist to realize the lift-off. There are two approaches to make a proper undercut for the lift-off. One approach is a wet etching process. In this process, O_2 plasma removes residues of the top layer resist while the etching developer, MF 319 solvent, creates an undercut in the bottom layer resist (Fig. 3.1). As an advantage the wet etching process does not affect the size of the holes. However, poor adhesion and difficulties to control process manually are the main disadvantages of this process. Another approach employs a dry etching process. This process uses RIE- O_2 plasma to realize a desired undercut in the resist. As a disadvantage this process affects the size of holes. In this work a dry etching process, which controls the diameter of the holes, is developed.

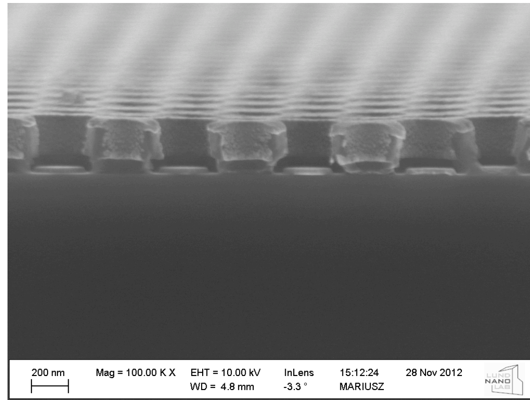

Figure 3.1: Cross sectional view of cavity produced by using a wet chemistry (MF319), after 30nm Au evaporation.

The development of the dry nanoimprint lift-off process is realized by a systematic study of the combination of double polymer layers as the imprinted material and plasma etching conditions of the polymers. In the first step after imprint, the top polymer layer has to be opened. In the second step, O_2 plasma is used to etch the bottom layer of the polymer. The purpose is to develop a technique based on all-dry etching to realize a required undercut in the bottom layer resist for the lift-off to deposit gold particles on the surface of substrate for growing of nanowire arrays. We have investigated the optimized RIE parameters, particularly the RIE etch time, enabling us to prepare the desired undercuts to deposit the gold particles. The growth of InP nanowire arrays from gold particles is carried out through epitaxial technique using MOVPE system and the properties of fabricated nanowire arrays are discussed. Finally, characterization is performed using the SEM and the ellipsometry.

3.1 IPS-STU NIL Lift-Off Process

As mentioned before, in order to pattern gold dots on the surface, the required undercut must be created for the lift-off process. Since the RIE etch time significantly affects the size of gold dots, this RIE parameter has been investigated. The processing steps to create gold particles are illustrated in Fig. 3.2.

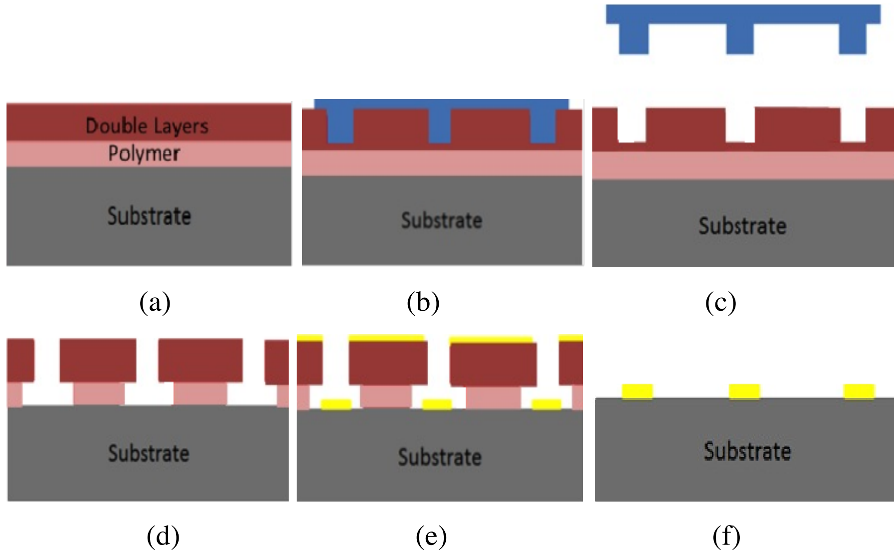

Figure 3.2: Schematic of processing steps to produce gold dots. (a) Si substrate coated with double layers resist, (b) NIL process, (c) Separation of the stamp leaving pattern on the resist, (d) O_2 plasma etching, (e) Metallization, (f) Lift-off process and depositing gold arrays on substrate.

3.1.1 Combination of Double Layer Resists

To prepare an undercut, a double polymer layers is used. After investigating and comparing the etch rate of different polymers, a combination of PMMA and TU7 was used. As discussed earlier, PMMA is a thermoplastic resist and is used as bottom layer resist. It has favorable properties such as the good adhesion and the uniform spin coating. The thermal stability during the metal evaporation, good stability when spinning the top layer and the fast etching rate in O_2 plasma etching. TU7 is a UV curable resist and has good imprint properties in Obducat IPS-STU process

and a high stability to O_2 plasma. First, a full 2 inch n-type Si (100) wafer is cleaned from organic compounds and any other contaminates, using acetone and isopropanol (IPA). The wafer is spin coated by PMMA 950k-A2 as the bottom layer by spin coating at 1500 rpm for 60 s and subsequently baked on a hotplate at 160 °C for 5 minutes. After cooling down, TU7 120K is deposited as the top layer by spin coating at 2500 rpm for 45 s and baking at 95 °C for 2 minutes. For details of the process see Appendix I.

3.1.2 IPS-STU Nanoimprint Process

First the nanoscale features of the Ni stamp as a master stamp is replicated into intermediate polymer stamp during the IPS process using NIL 6 inch system-Obducat. The master stamp supplied by Obducat AB having a pitch of 459 nm, a width of 230 nm and a height of 160 nm. To pattern the Si wafer which is spin coated by PMMA and TU7 with arrays of hole, the IPS is placed on top of the substrate while the simultaneous thermal and UV imprint is performed through STU recipe using NIL 6 inch system-Obducat (see Table 3.1 and Table 3.2 for IPS-STU process parameters).

Table 3.1: IPS process parameters

Temperature (°C)	Pressure (bar)	Post bake (s)
160	40	120

Table 3.2: STU process parameters

Temperature (°C)	Pressure (bar)	Post bake (s)	UV exposure (s)
75	20	120	10

After IPS-STU processing and transferring the structures into the wafer the imprinted wafer is inspected using the SEM. One example is shown in Fig. 3.3.

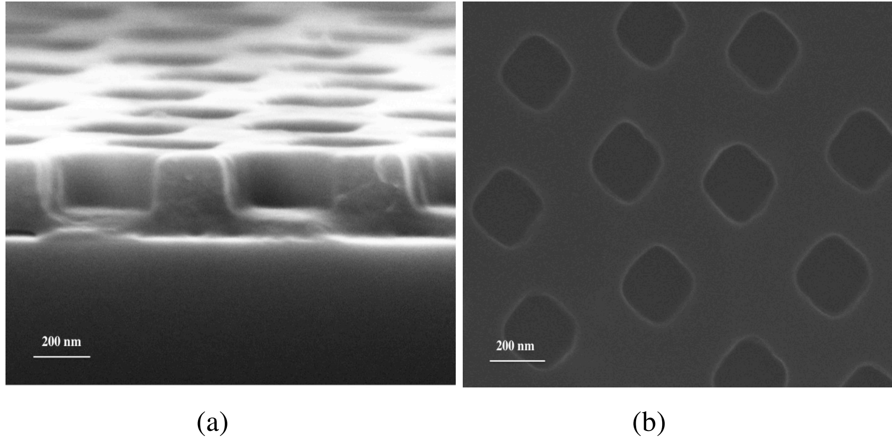

(a) (b)

Figure 3.3: SEM images after imprint. (a) Cross sectional view of patterned double layer resist on Si after IPS-STU process, (b) Top view of patterned substrate with hole arrays after IPS-STU process.

3.1.3 RIE-O_2 plasma

After the imprint process, the created holes in the top layer should be opened to get access to the bottom layer. High selectivity and anisotropy are the requirements for O_2 plasma etching. In this step, O_2 plasma is used to preferentially etch the bottom layer. Thus, the top layer has to be more stable in O_2 plasma and its stability determines the resolution. As described before, etch selectivity is the etch rate ratio between layers of a double layer resist and must be considerably larger than 1, ($\frac{R_2}{R_1}$>>1). In the O_2 plasma etching oxygen atoms and ions are reactive spices generated in the plasma. Oxygen ions attack the polymer layers and react with material atoms, leaving volatile precursors. Volatile precursors are removed by ion bombardment and the etching process is completed by transferring the pattern into the underlying polymer layer.

The basic reaction of the O_2 plasma with the polymers can be written as follow [4]

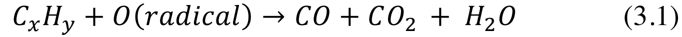

$$C_xH_y + O(radical) \rightarrow CO + CO_2 + H_2O \qquad (3.1)$$

The optimization of the RIE etch times is required to achieve the desired undercut into the underlying polymer layer as shown in Fig. 3.4. The imprinted wafer was cleaved into several pieces and the O_2 plasma etching was carried out at variable etching times of 70 s to 130 s, using Etcher RIE-Trion. The optimized O_2 plasma etching parameters are shown in Table 3.3.

Table 3.3: Optimized recipe for O_2 plasma etching for undercut making

Pressure (mTorr)	RIE-RF Power (W)	Flow O_2 (sccm)	Time (s)
150	40	40	80-120

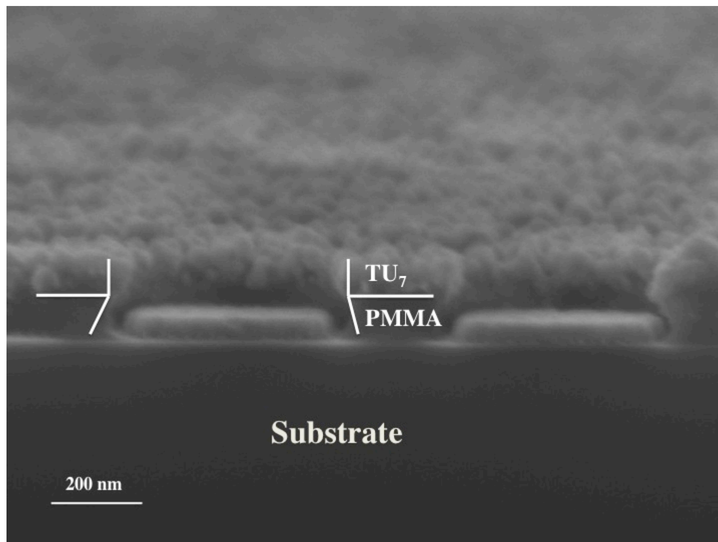

Figure 3.4: Cross sectional image of imprinted Si after undercut in a bottom layer resist, PMMA, by O_2 plasma etching.

3.1.4 Metallization and Lift–off

Metallization is performed by thermal evaporation of a 20 nm Au layer deposited using Evaporator-Pfeiffer 500. After the deposition, each piece of the sample is cut out into two parts, one for inspecting the cross-section and another one for investigating the produced undercuts versus the etch time using the SEM as shown in Fig. 3.5. The other parts are taken to perform the lift-off process.

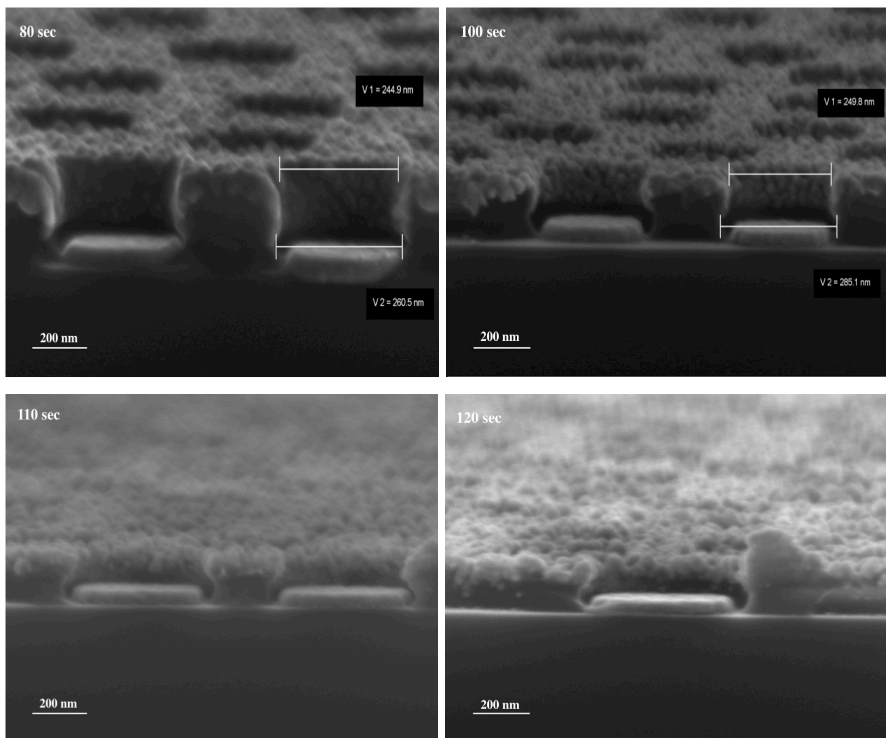

Figure 3.5: SEM images of undercut crating after Au 20 nm evaporation with different etch times varying from 80s to 120s by using O_2 plasma etching.

The lift-off is done to remove the excess metal and resist and to obtain the complete structure. The lift-off is performed by immersing the

remaining samples into the remover 1165 placed on a hot plate for approximately 5 minutes at 100 °C.

Afterwards samples are rinsed with IPA followed by blow drying with N_2. The top view SEM images of the samples were taken to investigate the properties of the patterned gold dots versus the etch time using SEM. As Fig. 3.6 shows, the control over the diameter of gold particles was achieved for etching times between optimized etch times of 80 s and 120 s.

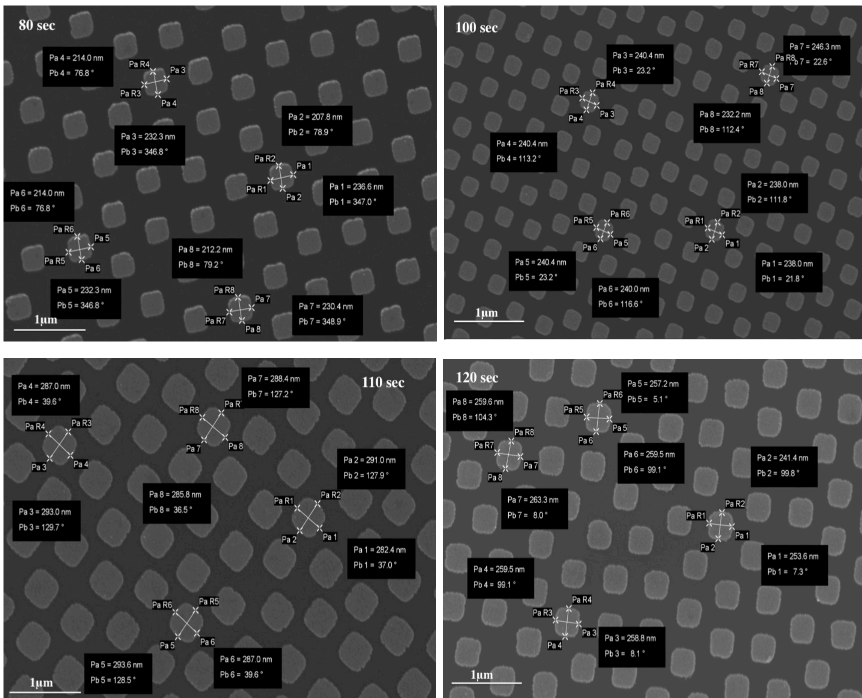

Figure 3.6: Top view of 20 nm Au dots with different etch times varying from 80 s to 120 s directly after lift-off.

3.2 Nanowire Growth

To fabricate the arrays of InP NW from gold particles (Fig. 3.7), first a 2 inch n-type InP (111) cleaned by using acetone and IPA is annealed at 200 °C for 5 minutes. Then the wafer is spin coated by PMMA 950k-A2 as the bottom layer by spin coating at 5500 rpm for 60 s and baked on a hotplate at 160 °C for 5 minutes. After cooling down, TU2 90K is deposited as top layer by spin coating at 1900 rpm for 60 s and baked at 95 °C for 2 minutes. See Appendix I for further details.

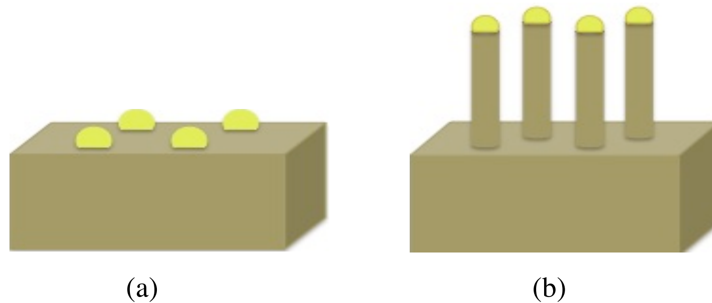

Figure 3.7: Schematic of growth of InP nanowires. (a) Gold seeded particles deposited on InP substrate by IPS-STU lift-off process, (b) Growth of InP nanowire arrays under gold particles.

Next, to define the pattern on a spin coated wafer, the structures of IPS is imprinted into the wafer. The IPS, which was replicated from a master stamp, is directly placed on top of the wafer by running a STU NIL recipe (Table 3.2), using NIL 6 inch system-Obducat. The used master stamp had hexagonal features with a pitch of 500 nm and a height of 120 nm.

After pattering, the imprinted sample is transferred to the RIE chamber in order to make the undercut in the bottom layer resist. O_2 plasma etching is performed using Etcher RIE-Trion at the etching conditions shown in Table 3.4.

Table 3.4: Recipe for O_2 plasma etching to prepare Au particles for growth

Pressure (mTorr)	RIE-RF Power (W)	Flow O_2 (sccm)	Time (s)
150	40	40	45

Since it was demonstrated that O_2 plasma used in dry etching process oxidizes the InP on the substrate [31], in order to remove the InP oxide on the substrate, the effect of a wet etching in chemical solutions such as HF and HCl is investigated. In this step the sample is cleaved into three pieces. One sample is taken without any treatment. Two other samples are treated by dipping into a diluted HF: H2O (1:50) for 20 s and a diluted HCl: H2O (1:10) for 30 s respectively, followed by rising in H_2O and drying by N_2 flow.

Metallization is carried out through the thermal evaporation method to deposit 20 nm of gold. Afterwards the unwanted resist is removed by performing lift-off for approximately 5 minutes in Remover 1165.

To grow the arrays of InP NW into the predefined position, the samples are then transferred to the MOVPE deposition chamber. Prior to the growth, the chamber is annealed at 550 °C for 10 minutes. Au particles act as catalyst. The precursors, Trimethylindium (TMIn) and Phosphine (PH_3) are inserted into the chamber at the temperature of 440 - 550 ° C for 1-10 minutes.

The arrays of InP nanowire are then grown on the substrate. The properties of grown NWs are investigated using the SEM. Also, the size distribution of grown NWs on the surface is analyzed by using Image J program.

3.3 Characterization Method

Two main characterization methods were used in the present work: the scanning electron microscopy (SEM) and the spectroscopic ellipsometry. The SEM technique was used to characterize the nanoscale features after the RIE and the lift-off process and also, for the inspection of nanowires. The ellipsometry was used to determine the thickness of the resist layers deposited by spin coating.

3.3.1 Scanning Electron Microscopy

Scanning electron microscopy (SEM) is a high precision microscopy that uses an electron beam to probe the sample in a raster pattern. A very high magnification up to 500,000 times is achievable by the SEM. The resolution, depends on the size of the electron spot, the size of the probed volume and the interaction of the specimen with the electron beam. Since the two first parameters are larger than atomic distances, the resolution is limited to about less than 1 nm.

An electron beam is produced by a thermionic or a field emission electron gun. Then, this beam is focused and controlled by electro-magnetic lenses. The scanning coils deflect the beam to scan the sample in a raster pattern.

As a result of the interaction of the beam with the sample, three phenomena happen: elastic scattering of electrons, inelastic backscattering of secondary electrons with the energy lower than primary ones and the emission of X-rays. Each of these signals can be detected by a special detector. The secondary electron (SE) detector provides topographic information of the surface of the sample; however, the composition of the specimen is determined by the backscattered electrons and X-rays [28].

3.3.2 Ellipsometry

To characterize the film thickness and the optical constants such as the refractive index, ellipsometry is used. When the light reflects from the substrate a change in polarization of light is accrued which is measured using ellipsometry. The change in polarization is demonstrated as an amplitude ratio, ψ, and the phase difference Δ. Ellipsometry is also used to determine other material properties such as composition, roughness, doping concentration, associated with an optical response change [29].

CHAPTER 4
Results and Discussion

4.1 Investigation of Etch Rate

To make undercut in a bottom polymer layer for the lift-off high etch selectivity of double polymer layer is required. To achieve high selectivity the bottom layer must have the fast etch rate in O_2 plasma while the top layer must be stable in O_2 plasma. As a possibility of combination of double polymer layers, first the etch rate of PMMA with different molecular weight and TU2 was investigated. The etch rate is dependent on O_2 plasma parameters such as pressure, flow of O_2 and RIE-RF power. In the first group to etch away the deposited polymer materials on plain Si separately, O_2 plasma was used with the starting parameters: The pressure of 150 mTorr, the O_2 flow of 40 sccm and the RIE-RF power of 25 W and the etch time of 60 s.

In the second group including PMMA 950 k-A2 and TU7 120k, O_2 plasma was used with the pressure of 150 mTorr, the O_2 flow of 40 sccm and the RIE-RF power of 40 W and the etch time of 60 s. The etch rate of each polymer was obtained by measuring the thickness of polymer layers before and after plasma etching using the ellipsometer (see Table 4.1 and Table 4.2). The etch rate test results indicated that PMMA 950 k-A2 has a higher etch rate in O_2 plasma in comparison with others PMMA, and it was chosen as the bottom polymer layer against TU7 as the top layer.

Table 4.1: Etch rate of PMMA with different molecular weight and TU2 (Etching condition: pressure of 150 mTorr, flow O_2 of 40sccm, RIE-RF power of 25 W and etch time of 60 s).

Resist	PMMA 50 k-A5	PMMA 950 k-A6	PMMA 200k-A5.5	TU2
Etch rate (nm/min)	13.8	19.6	14.5	8.6

Table 4.2: Etch rate of PMMA950 k-A2 and TU7 (Etching condition: pressure of 150 mTorr, flow O_2 of 40sccm, RIE-RF power of 40 W and etch time of 60 s).

Resist	PMMA 950 k-A2	TU7
Etch rate (nm/min)	111.4	65

4.2 Dry Etching Process Results of NIL Samples

The possibility of having the desired undercut by using O_2 plasma etching was studied. In initial experiments O_2 plasma was used with the starting pressure of 150 mTorr, the O_2 flow of 40 sccm, the RIE-RF power of 25 W and the etch time of at least 10 minutes.

SEM images demonstrated no cavity making in the bottom layer (see Fig. 4.1). Therefore it was essential to change and optimize the RIE parameters to make proper undercuts for the lift-off.

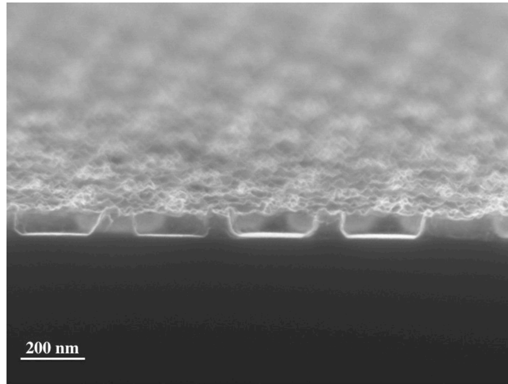

Figure 4.1: SEM image of cross section after Au 20 nm evaporation; no cavity making using O_2 plasma etching with pressure of 150 mTorr, flow O_2 of 40 sccm, RIE-RF power of 25 W and etching time of 14 minutes.

By increasing the O_2 flow and at different etch times between 70 s and 130 s, an optimized recipe for O_2 plasma etching dependent on RIE parameters was obtained (Table 3.3). SEM images exhibited that the required undercuts for the lift-off were realized at optimized etching times of 80 s to 120 s. No undercut formed at the etching times below 80 s. But at the etch time higher than 120 s the resists were completely destroyed (Fig. 4.2).

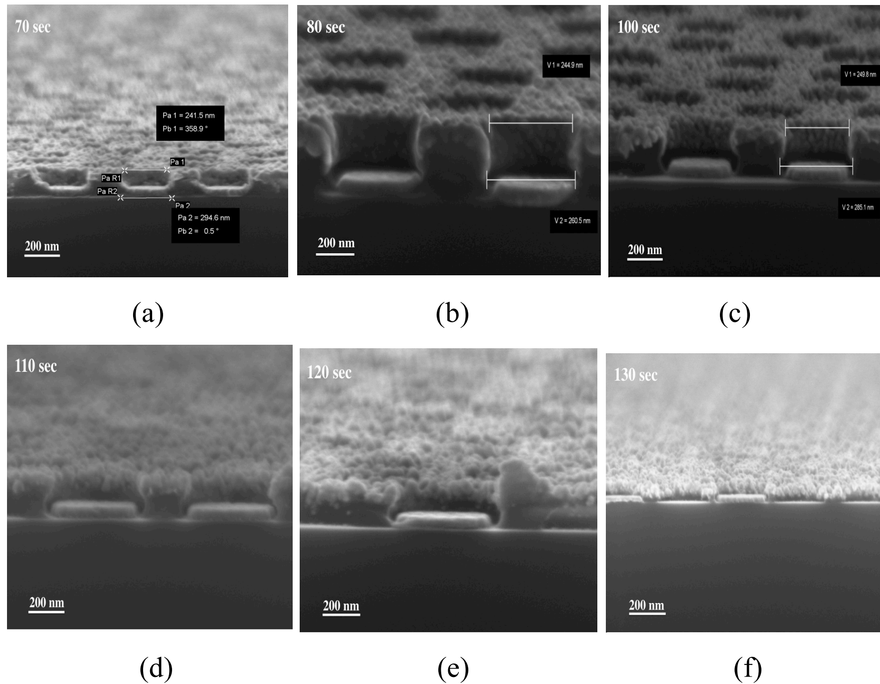

Figure 4.2: SEM images of profiles after Au 20 nm evaporation on imprinted substrate. Driving varying etch times of 70 s-130 s using O_2 plasma etching with pressure of 150 mTorr, flow O_2 of 40 sccm, RIE-RF power of 40 W results (a) No undercut making at etch time of 70 s, (b), (c), (d), (e) Required undercuts appeared at etch times of 80 s to120 s. (f) At etch time of 130 s resist is completely gone.

4.3 Lift-off Process Results

The target of this work was to define the gold particles on an imprinted substrate with a controlled dimension after the lift-off process. The SEM inspection indicated that the controlled diameter of Au particles could be obtained after O_2 plasma etching for the optimized etch times of 80 s to 120 s. In some experiments, which were not within optimized ones, the lift-off process was unsuccessful.

The remover solvent used for the lift-off washed away everything resulting in missing a lot of metal dots. In some other experiments the lift-off was not performed since for higher etch time the erosion of TU7 makes rests of resist so cross link and stick to the bottom layer resist, PMMA and Si substrate so it is impossible to dissolve (Fig. 4.3).

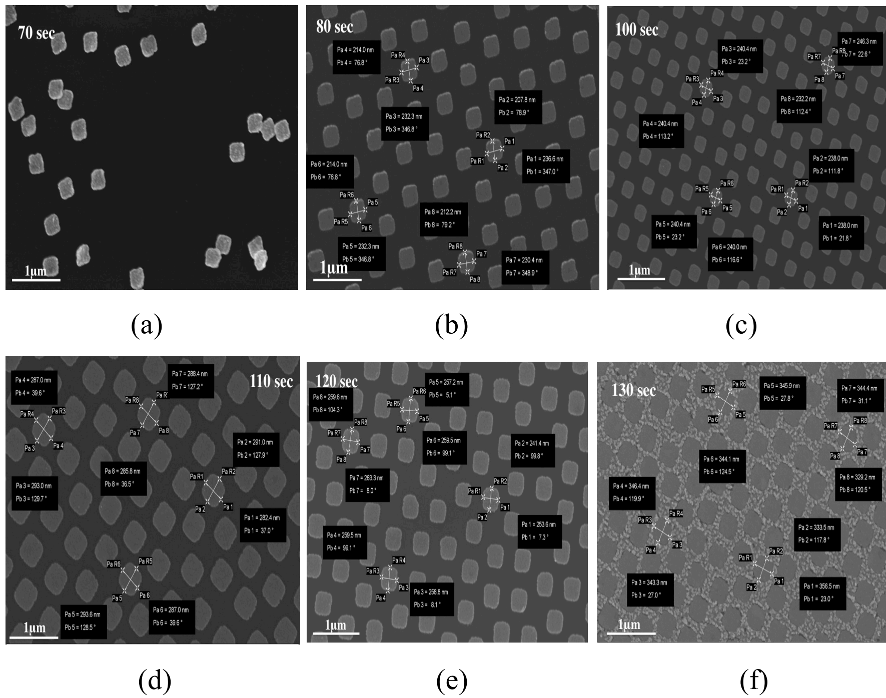

Figure 4.3: Top view images of 20 nm Au dots on Si after lift-off. (a) Missing of gold dots at etch time of 70s, (b), (c), (d), (e) Deposition of gold dots in defined position at etch times of 80 s to120 s, (f) Non lifting metal at etch time of 130 s.

The optimized experiments demonstrated high lift-off yield; only small areas remained with non-lifting metal. The diameter of gold dots was increased almost linearly with the etching time. The experiments proved good reproducibility.

4.4 Nanowire Growth Results

The gold particles defined by IPS-STU lift-off process were used to grow the InP nanowire arrays. After the growth, the SEM images revealed that the dry etching process works well for the growth of InP NWs. The SEM inspection also indicated that the gold particles tend to move on the surface and merge together during the epitaxial growth which leads to larger diameters of grown NWs (Fig. 4.4 b). In order to decrease the merging phenomena of the gold particles on a plasma oxidized surface of InP [31], the influence of the wet chemical treatment after the O_2 plasma etching on the growth of nanowires was investigated. As discussed in chapter 3.2, a diluted HF solution and a diluted HCl solution were used separately to remove the InP oxide formed after the O_2 plasma etching. The SEM inspection after the NW growth indicated that on the HF treated surface, the smallest number of particles were moved around and merged together resulting in a nearly uniform InP NW growth; almost all the nanowires were grown at the predefined positions in comparison to the HCl treatment (Fig. 4.4). However, to control the quality and the position of NWs, the effect of varying thickness of the gold layer deposited on the imprinted pattern and the influence of a thermal annealing step at a high temperature prior to the growth were reported [30].

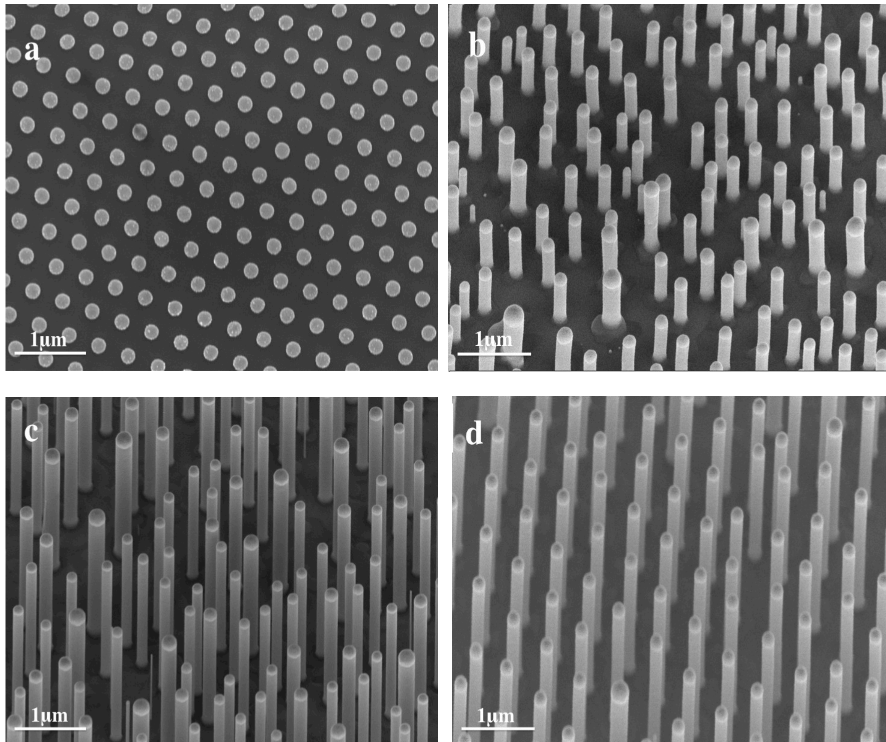

Figure 4.4: (a) 20 nm Au dots directly after lift-off on InP, prior to the growth of nanowires, (b) Nanowire arrays on the non-treated surface with undesired nanowires growth, (c) Nanowire arrays on the HCl treated surface, (d) Influence of HF treatment on the surface results in desired nanowires growth.

Figure 4.5 shows the results of IPS-STU lift-off process using the wet chemical etching and growth of nanowires. In comparison with dry etching the smallest movement of the gold particles and subsequently better growth of nanowires with controlled dimensions could be realized on non-treated InP substrate using wet chemistry to make the undercut in the NIL resist.

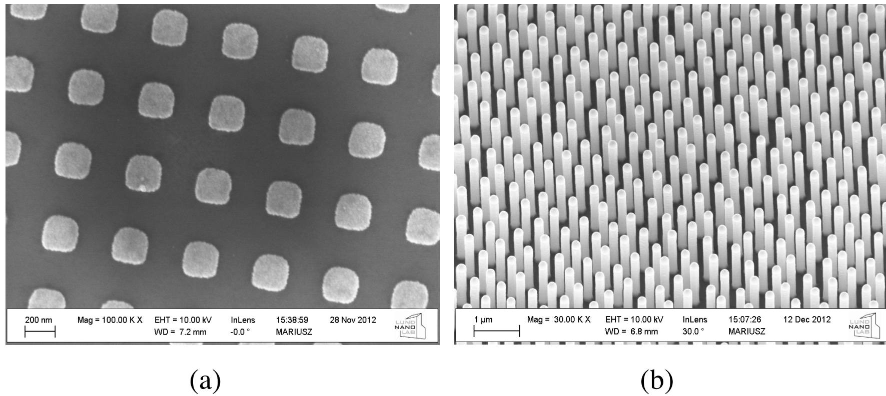

(a) (b)

Figure 4.5: (a) Front view of Au 30nm dots on InP substrate directly after lift-off, (b) Non treated InP substrate after growth by using wet chemical etching for creating an undecut in the resist.

To see how these treatments affect the growth of NWs, the distribution of grown nanowires on InP substrate was determined using Image J program. To analyze, the top view SEM images of non treated and treated substrates after growth with magnification of 5.00 K X was used. By using Image J program the area of particles was measured. The data was imported to the MATLAB program and the diameter of particles versus the density of particles was plotted as a histogram. As shown in Fig. 4.6 the diagrams show a Gaussian distribution. The distribution of grown NWs on non-treated substrate exhibits an asymmetric peak corresponding to the largest merging of gold particles during the epitaxial growth (Fig. 4.6 a). The distribution of NWs on the HCl treated substrate indicates several peaks corresponding to the merging of a number of particles together (Fig. 4.6 b). Finally, the distribution of NWs on the HF treated substrate demonstrated a much better distribution (Fig. 4.6 c). This peak corresponds to the smallest movement and merging of gold particles on the InP substrate treated by HF and consequently a much better controlled growth of NWs.

The diameters of gold dots directly after lift-off were measured in the range of 200 nm to 240 nm. The histogram c shows that the majority of NWs were grown in this interval.

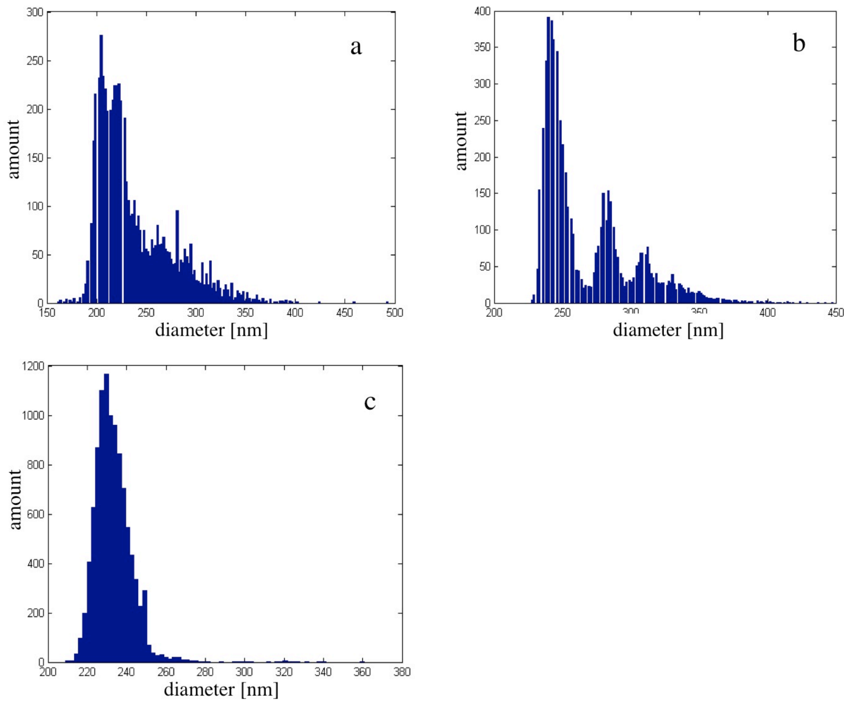

Figure 4.6: Size distribution of InP nanowires. (a) Distribution of grown InP nanowires on non treated substrate, indicating that a lot of gold dots merged together and a big movement of particles, (b) The movement of gold particles is still observable on HCl trated substrate, (c) The smallest merging of gold particles was seen on treated substrate by HF and InP nanowires grew on controlled positions.

CHAPTER 5
Conclusions and Outlook

In this work, a dry etching process to make the undercut for the lift-off was developed and compared to the conventional wet chemical etching process. The IPS-STU NIL process was applied for defining the gold particles as seeds for subsequent NW growth. To achieve a high etch selectivity, the etch rate of possible polymer layers was investigated and a best combination of double polymer layers was selected. By optimizing RIE-O_2 plasma parameters such as the O_2 flow, the RIE-RF power and the etch time, the desired undercuts appeared for etch times between 80 s and 120 s. After the lift-off, gold particles were produced with a controlled diameter between optimized etch times.

InP nanowires were grown from gold particles using metal-organic vapour phase epitaxy. It was demonstrated that, due to the presence of InP oxide induced by O_2 plasma on the substrate, gold particles tend to move and merge together during the epitaxial growth. The effects of the wet

chemical etching to remove the InP oxide after O_2 plasma etching was investigated by using the HF solution and the HCl solution. The influence of the diluted HF solution to remove the InP oxide on the surface resulted in the least movement and merging of the gold particles and a more uniform InP NW growth on the predefined positions compared to that treated by the diluted HCl solution.

As a further study it is suggested to find the process windows for different geometries of the stamp. Furthermore, the characteristics of the NWs grown using the dry etching can be compared to those grown using the wet etching.

APPENDIX I

Table I.1 shows resist deposition parameters applied in IPS-STU lift-off process to make undercut for the lift-off. First polymer layer is PMMA 950k-A2 and second polymer layer is TU_7 120k deposited on a 2 inch Si (100) substrate.

Table I.1: Resist deposition parameters in order to create undercut for the lift-off.

Substrate	Resist	Spin speed (rpm)	Spin time (s)	Post bake (°C)	Post bake time (min)
Si (100)	PMMA 950k-A2	1500	60	160	5
	TU_7 120k	2500	45	95	2

Table I.2 shows resist deposition parameters performed in IPS-STU lift-off process in order to prepare gold particles to growth of nanowires. The first layer is PMMA 950k-A2 and the second layer is TU_2 90k spin coated on a 2 inch InP (111) substrate annealed at 200 °C for 5 minutes.

Table I.2: Resist deposition parameters in order to prepare gold particles for growth of nanowires.

Substrate	Resist	Spin speed (rpm)	Spin time (s)	Post bake (°C)	Post bake time (min)
InP (111)	PMMA 950k-A2	5500	60	160	5
	TU_2 90k	1900	60	95	2

Bibliography

[1] Z. Cui, "Nanofabrication Principals, Capability and Limits", Springer Science, Business Media, LLC, 2008.

[2] L. Jay. Guo, "Nanoimprint Lithography: Methods and Material Requirements", Adv. Mater. 2007, 19, 495-513.

[3] L. Jay. Guo, "Recent Progress in Nanoimprint Technology and Its Application", J. Phys. D: Appl. Phys. 37 (2004), R123-R141.

[4] H. Abe, M. Yoneda, N. Fujiwara, "Development of Plasma Etching for Fabricating Semiconductor Devices", Japanese Journal of Applied Physics, Vol. 47, No. 3, 2008, pp. 1435-1455.

[5] L. R. Harriot, "Limits of Lithography", Proceeding of the IEEE, Vol. 89, No. 3, 2001.

[6] J. Viheriälä, T. Niemi, J. Kontio, M. Pessa, "Nanoimprint Lithography-Next Generation Nanopattering Methods for Nanophotonics Fabrication", Recent Optical and Photonic Technologies, Book edited by: K. Y. Kim, 978-953-7619-71-8, pp. 450, 2010.

[7] "Optical Lithography", Copy right © 2004, www.SiliconFarEast, from http://www.siliconfareast.com/lith_optical.htm.

[8] M. Tarequzzaman, "Nanoimprint Lithography Applications of Metal Assisted Chemical Etching of Silicon", Thesis for Master of Science in Physics, Lund University, 2013.

[9] C. Vieu, F. Carcenac, A. PePin, C. M. Mejias, "Electron Beam Lithography: Resolution Limits and Applications", Applied Surface Science 164 (2000), 111-117.

[10] K. K. Likharev, Proceedings of the IEEE 87(1999) 606.

[11] A. E. Grigorescu, C. W. Hagen, "Resists for Sub-20-nm Electron Beam Lithography: state of the art. 2009 Nanotechnology 20 292001.

[12] "SPIE Handbook of Microlithography, Micromachining and Microfabrication", Cornell NanoScale Science & Technology Facility (CNF), http://www.cnf.cornell.edu/cnf_spie1.html, accessed in 2012.

[13] W. Zhou, G. Min, J. Zhang, Y. Liu, “Nanoimprint Lithography: A Processing Technique for Nanofabrication Advancement”, Nano-Micro Lett. 3 (2), 135-140 (2011).

[14] E. A. Costner, M. W. Lin, W. L. Jen, C. G. Willson, Nanoimprint Lithography Materials Development for Semiconductor Device Fabrication, Annu. Rev. Mater. Res. 2009. 39:155-80.

[15] S. Lundahl, “Nanoimprint Lithography: An Investigation of Its Use Today in Relation to the Past”, Nanovation Internship Program, Lund University, Report 4-2011.

[16] M. Meier, “Nanoimprint Lithography for Crossbar Arrays”, 2011, from http://www.emrl.de/r_m_1.html.

[17] A. P. Nayak, L. VJ, M. Saif Islam, “Wet and Dry Etching” University of California,<http://www.ece.ucdavis.edu/~anayakpr/Papers/Wet%20and%20Dry%20Etching_submitted.pdf>

[18] S. M. Irving, Proc. Kodak Photoresist Seminar 2, 1968, p. 26.

[19] S. M. Irving, Solid State Technol. 14 (1971) 47.

[20] S. M. Sze, “Physics of semiconductor Devises”, 2nd ed. Wiley, 1981.

[21] N. Hosokawa, R. Matsuzaki, T. Asmaki, Proc. 6th Int.Vacumm Conger., Kyoto, 1974, Jpn. J. Appl. Phys. 2 (1974) Suppl. 2-1, p.435.

[22] A. Grill, “Cold Plasma in Materials Fabrication”, IEEE, 1994.

[23] Liberman, Lichtenberg, “Principle of Plasma Discharges and Materials Processing”, Wiley-Interscience , 1994.

[24] M. Yazawa et al, “Hetroepitaxial Ultrafine Wire-like Growth of InAs on GaAs Substrates”, Appl. Phys. Lett., vol. 58, no. 10, pp. 1080-1082, 1991.

[25] K. Hillerich, “Inflience of Seed Particle Material, Preparation, and Dynamics on Nanowire Growth”, Doctoral thesis, Lund University, 2013.

[26] J. Bolinsson, “The Crystal Structure of III-V Semiconductor Nanowires: Growth and Characterization”, Doctoral thesis, Lund University, 2010.

[27] J. Wallentin et al, “InP Nanowire Array Solar Cells Achieving 13.8% Efficiency by Exceeding the Ray Optics Limit”, Science, 339, 1057 (2013).

[28] J. Atteberry, “How Scanning Electron Microscopes Work,” 21 April 2009, HowStuffWorks.com <http://science. Howstuffworks.com/scanning-electron-microscope.htm> 04 February 2012.

[29] J. A. Woollam Co, “Spectroscopic Ellipsometry Tutorial Introduction “, © 2013 J. A. Woollam Co, <http://www.jawoollam.com/tutorial_1.html>

[30] U. Krishnamachari, M. Borgstrom, B. J. Ohlsoon, L. Samuelson, “Defect-Free InP Nanowires Grown in [001] Direction on InP (001)”, Appl. Phys. Lett, 85, 2077 (2004); doi: 10.1063/1.1784548.

[31] R. Jafari Jam et al., “Nanoimprint Lithography and Gold Electroplating for Nanowire Seed Particle Definition”, The 12th international conference on nanoimprint and nanoprint technology, Barcelona, Spain, 2013.

[32] “Photolithography”, <http://www.ece.gatech.edu>.